Estimating Turbulent Heat Fluxes With a Weak-Constraint Data Assimilation Scheme: A Case Study (HiWATER-MUSOEXE)

Tongren Xu, S. Mohyddin Bateni, and Shunlin Liang, *Fellow, IEEE*

***Abstract*—A weak-constraint variational data assimilation (WC-VDA) scheme was developed to estimate turbulent heat fluxes by assimilating sequences of land surface temperature measurements. In contrast to the commonly used strong-constraint VDA system, the WC-VDA approach accounts for the effects of structural and model errors and generates better results. This is achieved by adding a model error term (ω) to the surface energy balance equation. The WC-VDA model was tested at two sites with very distinct hydrological and vegetated conditions: the Daman site (a wet site located in an oasis area and covered by seeded corn) and the Huazhaizi site (a dry site located in a desert area and covered by sparse grass). The two sites represent typical desert–oasis landscapes in the middle reaches of the Heihe River Basin, northwestern China. The results proved that the WC-VDA method performed well over very dry and wet conditions, and the estimated sensible and latent heat fluxes agree well with eddy covariance measurements.**

***Index Terms*—Evapotranspiration, land surface temperature (LST), latent heat flux, sensible heat flux, weak-constraint variational data assimilation (WC-VDA).**

I. Introduction

THE magnitude of turbulent heat fluxes, particularly latent heat flux (LE), is the most important component of the water cycle in arid regions. Flux towers have been established to measure turbulent heat fluxes across the world [1]–[3]. However, flux tower stations are sparsely distributed on different continents and have only measured surface fluxes over a limited time period because these measurements are expensive and difficult. Consequently, a number of models have been developed to estimate turbulent heat fluxes in a more convenient way.

Land surface temperature (LST) is an important variable in land surface energy balance (SEB) processes [4], and it has been effectively estimated from satellite observations [5]. With LST data, different models for the retrieval of turbulent heat fluxes can be divided into three main groups. In the first group, turbulent heat fluxes can be obtained using the empirical relationships between the LST and vegetation indexes [6], [7]. The second group estimates turbulent heat fluxes by solving the SEB equation [8]–[10]. Both groups can estimate turbulent heat fluxes at the regional scale, but they are not able to generate temporally continuous surface heat fluxes. In fact, these two groups of methods can only obtain surface heat fluxes for instances in which LST observations are available.

The third group estimates turbulent heat fluxes by assimilating LST observations into the SEB equation or land surface models [11]–[22]. This group takes advantage of the significant amount of information contained in the temporal variations of LST measurements and estimates surface heat fluxes even for instances in which LST observations are not available. By assimilating the sequences of LST observations, the SEB equation can be resolved by optimizing its two key unknown parameters, i.e., neutral bulk heat transfer coefficient (C_{HN}) and evaporative fraction (EF). C_{HN} scales the sum of turbulent heat fluxes, and EF scales their partitioning. The variational data assimilation (VDA) scheme utilizes the force-restore equation as the constraint [11]–[17]. However, the force-restore equation is simple, parsimonious, and can lead to erroneous surface heat flux predictions [18]. Recently, the VDA scheme has been significantly advanced by using the full heat diffusion equation as a physical constraint instead of the force-restore equation to improve the surface heat flux estimates [18]–[20].

Most studies in the third group used "strong-constraint" VDA (SC-VDA) schemes that assume that the model structure is perfect and that the input data are not noisy. However, there are many uncertainties in the model structure and input variables. The inclusion of model error term (ω) gives the VDA scheme the ability to capture the errors caused by the model structure and the noisy data. Thus, in this letter, a weak-constraint VDA (WC-VDA) scheme is used to capture errors in the SEB equation. The WC-VDA system does not allow the errors to adversely affect the optimization scheme, and it improves the surface heat flux estimates.

This letter is conducted over the middle reach of the Heihe River Basin (HRB), which is located in northwestern China. The HRB is an inland river basin, and a desert–oasis system constitutes the typical land surface features of the middle reach. Moreover, the oasis system consumes a considerable amount of HRB water, and the magnitude of the Heihe River water consumption is crucial to local agricultural economics.

Manuscript received January 25, 2014; revised March 28, 2014 and May 5, 2014; accepted May 15, 2014. This work was supported in part by the National Natural Science Foundation of China (91125002 and 41201330), the High-Tech Research and Development Program of China (No. 2013AA121201), and Water Resources Research Institute at the University of Hawaii.

T. Xu is with the State Key Laboratory of Remote Sensing Science, Research Center for Remote Sensing and GIS, and School of Geography, Beijing Normal University, Beijing 100875, China (e-mail: xutr@bnu.edu.cn).

S. M. Bateni is with the Department of Civil and Environmental Engineering and Water Resources Research Center, University of Hawaii at Manoa, Honolulu, HI 96822 USA (e-mail: smbateni@hawaii.edu).

S. Liang is with the State Key Laboratory of Remote Sensing Science, and College of Global Change and Earth System Science, Beijing Normal University, Beijing 100875, China and also with the Department of Geographical Sciences, University of Maryland, College Park, MD 20742 USA (e-mail: sliang@umd.edu).

Digital Object Identifier 10.1109/LGRS.2014.2326180

II. Methodology

A. Heat Diffusion Equation

The ground temperature at a depth of z and at time t, i.e., $T(z,\, t)$, is given by the heat diffusion equation as

$$c\frac{\partial T(z,\, t)}{\partial t} = \frac{\partial}{\partial z}\left(\lambda \frac{\partial T(z,\, t)}{\partial z}\right) \tag{1}$$

where c and λ are the soil volumetric heat capacity [in $(\mathrm{J}\cdot \mathrm{m}^{-3}\cdot \mathrm{K}^{-1})$] and the thermal conductivity [in $(\mathrm{W}\cdot \mathrm{m}^{-1}\cdot \mathrm{K}^{-1})$], respectively.

To solve the heat diffusion equation, its boundary conditions at the top and bottom of the soil column need to be specified. The boundary condition at the top of the soil column, i.e., $T(z=0,\, t)$, is retrieved from the surface boundary forcing equation, i.e., $\lambda\, dT(0,\, t)/dz = -G(0,\, t)$. The soil temperature at a depth of 0.3–0.5 m is almost invariant over a day [23]. Therefore, a Neumann boundary condition is used at the bottom of the soil column, i.e., $dT(z = 0.5\ \mathrm{m})/dz = 0$.

B. SEB Equation

The SEB equation with model uncertainty (ω) can be written as

$$G(0,\, t) = R_n - H - LE - \omega(t) \tag{2}$$

where R_n is the net radiation [in $(\mathrm{W}\cdot \mathrm{m}^{-2})$], H and LE are the sensible and latent heat fluxes [in $(\mathrm{W}\cdot \mathrm{m}^{-2})$], respectively, and $\omega(t)$ is an unknown model error term. It is added to the SEB equation to account for the model and observation errors. The calculation of R_n can be found in [18].

Sensible heat flux (H) can be calculated via

$$H = \rho_a c_p C_H U(T - T_a) \tag{3}$$

where ρ_a is the air density [in $(\mathrm{kg}\cdot \mathrm{m}^{-3})$], c_p is the heat capacity of air ($1012\ \mathrm{J}\cdot \mathrm{kg}^{-1}\cdot \mathrm{K}^{-1}$), U and T_a are the wind speed [in $(\mathrm{m}\cdot \mathrm{s}^{-1})$] and the air temperature (in kelvins), respectively, and C_H is the bulk heat transfer coefficient (-). Bulk heat transfer coefficient (C_H) mainly depends on landscape conditions and atmospheric stability. Bulk heat transfer coefficient C_H is related to neutral bulk heat transfer coefficient (C_{HN}) and stability correction function (f) via [13]

$$C_H = C_{HN} f(\mathrm{Ri}) = C_{HN}\left[1 + 2(1 - e^{10\mathrm{Ri}})\right] \tag{4}$$

C_{HN} depends on the geometry of the land surface, varies on the time scale of vegetation phenology (monthly), and constitutes the first unknown parameter of the WC-VDA scheme [13]–[15], [17]–[20]. Ri is the Richardson number and is obtained according to the work in [14].

Evaporative fraction (EF) is the second unknown parameter of the WC-VDA scheme and is almost constant for the near-peak radiation hours on days without precipitation [24]. It can be defined as

$$EF = \frac{LE}{(H + LE)}. \tag{5}$$

Latent heat flux (LE) can be obtained via

$$\frac{LE}{H} = \frac{\mathrm{EF}}{1 - \mathrm{EF}}. \tag{6}$$

This letter uses a big leaf approach as LE in (6) is the total latent heat flux from the bulk canopy and soil and not from a single leaf and soil.

C. Cost Function

To estimate unknown parameters (C_{HN} and EF) and model error term (ω) in the WC-VDA scheme, cost function J is defined as follows:

$$\begin{aligned} J(T, R, EF, \Lambda, \omega) = & \sum_{i=1}^{N=30} \int_{t_0=0900}^{t_1=1800} \left[T_{\mathrm{obs},i}(t) - T_i(t)\right]^T \\ & \times K_T^{-1}\left[T_{\mathrm{obs},i}(t) - T_i(t)\right] dt \\ & + (R - R')^T K_R^{-1}(R - R') \\ & + \sum_{i=1}^{N=30} \left(EF_i - EF_i'\right)^T K_{EF}^{-1}\left(EF_i - EF_i'\right) \\ & + 2\sum_{i=1}^{N=30} \int_{t_0=0900}^{t_1=1800} \int_{0}^{l=0.5} \Lambda_i(z,t) \\ & \times \left[c\frac{\partial T_i(z,t)}{\partial t} - \frac{\partial}{\partial z}\left(\lambda \frac{\partial T_i(z,t)}{\partial z}\right)\right] dz dt \\ & + \sum_{i=1}^{N=30} \int_{t_0=0900}^{t_1=1800} \int_{t_0=0900}^{t_1=1800} \\ & \times \omega_i(t') K_\omega^{-1}(t', t'') \omega_i(t'') dt' dt''. \end{aligned} \tag{7}$$

The first term on the right-hand side of the cost function represents the misfit between LST observations (T_{obs}) and model predictions (T) over the whole data assimilation period $(N = 30$ days). The assimilation window of [0900–1600 local time] is used, for which EF is assumed to be invariant. To make C_{HN} always positive and physically meaningful, it is related to R via $C_{HN} = \exp(R)$. R' and EF' are prior estimates (their initial values are specified for the first iteration). The second and third terms represent the misfit between the R and EF estimates and their prior values, respectively. C_{HN} is assumed to be constant over the entire monthly assimilation period $(N = 30$ days). The data assimilation scheme finds the optimum values of R and EF by minimizing the difference between the LST observations and the predictions. Following the work in [18], R' and EF' are set to -5 and 0.7, respectively. K_T^{-1}, K_R^{-1}, and K_{EF}^{-1} are constant numerical parameters and are set to 0.01 K^{-2}, 1000, and 1000, respectively [18]. For detailed information on the impact of K_T^{-1}, K_R^{-1}, and K_{EF}^{-1} on the performance of the model, see [18].

The fourth term is the heat diffusion equation, which is adjoined to the cost function (as a physical constraint) via Lagrange multiplier Λ. l is the depth of the bottom boundary condition and is set to 0.5 m [18], [20], [23]. The last term

accounts for model error $(\omega(t))$ and minimizes the deviation from the prior value. Following the works in [25] and [26], an exponential structure for the model error covariance is used as follows:

$$K_{\omega}^{-1}(t',\, t'') = \sigma_{\omega}^{2} \exp\left(|t' - t''|/\tau\right) \tag{8}$$

where σ_{ω} is the standard deviation of the model error ($100\ \mathrm{W \cdot m^{-2}}$ in this letter), and τ is the decorrelation time scale (6 h in this letter) [18]. This kind of error covariance model is typically used when the covariance structure of errors is poorly known. The optimal values for C_{HN}, EF, and ω are obtained by minimizing the cost function (i.e., setting its first variation equal to zero, i.e., $\delta J = 0$). Setting $\delta J = 0$ leads to a number of equations (called the Euler–Lagrangian equations) that should be solved simultaneously. See [18] for a complete set of the Euler–Lagrangian equations.

III. Data Sets

The WC-VDA scheme is tested at two sites in the middle reach of the HRB, northwestern China: One site is an oasis site that is covered by seeded corn (a wet/densely vegetated site), and the other is a desert site that is covered by grass (a dry/sparely vegetated site). The oasis and desert sites are called Daman and Huazhaizi, respectively. These sites with distinct hydrological and vegetated land surfaces represent the typical land characteristics of the HRB. The data used in this letter are sourced from the Multi-Scale Observation Experiment on Evapotranspiration over heterogeneous land surfaces of the Heihe Water Allied Telemetry Experimental Research (HiWATER-MUSOEXE) [3], [27].

The sensible and latent heat fluxes are measured by an eddy covariance (EC) instrument and are used to validate the WC-VDA estimates. The methods of data processing and quality control of turbulent heat flux data can be seen in [1] and [2]. All the micrometeorological and flux data were measured every 30 min. The model was run in 30-min time steps during Julian days 159–248 in 2012.

Soil volumetric heat capacity (c) and thermal conductivity (λ) are set to 2.43×10^{6} $(\mathrm{J \cdot m^{-3} \cdot K^{-1}})$ and 1.99 $(\mathrm{W \cdot m^{-1} \cdot K^{-1}})$ at the Daman site. The corresponding values are 1.76×10^{6} $(\mathrm{J \cdot m^{-3} \cdot K^{-1}})$ and 1.33 $(\mathrm{W \cdot m^{-1} \cdot K^{-1}})$, respectively, at the Huazhaizi site. These values are obtained based on the soil texture and moisture measurement at these sites [28]–[30].

The micrometeorological data (including wind speed, air temperature, and incoming shortwave radiation), LST observations, and soil thermal properties constitute the inputs of the WC-VDA system.

IV. Results

C_{HN} and EF are two key parameters in the SEB scheme, as explained in Section II. These two parameters are obtained via the WC-VDA framework. The C_{HN} parameter is estimated for each 30-day period, and the EF parameter is estimated for each day [14].

At the Daman site, the estimated C_{HN} values are 2.5×10^{-3}, 7.5×10^{-3}, and 6.9×10^{-3} in monthly periods 159–188, 189–218, and 219–248, respectively. The corresponding C_{HN} estimates are 1.6×10^{-3}, 1.9×10^{-3}, and 1.8×10^{-3} at the Huazhaizi site. The measured leaf area index (LAI) values in the three monthly periods are 2.2, 4.3, and 3.3 $\mathrm{m^2 m^{-2}}$ for the Daman site (0.2, 0.3, and 0.3 $\mathrm{m^2 m^{-2}}$ for the Huazhaizi site). The changes in the estimated C_{HN} values are consistent with the variations in the LAI at both sites. For example, at the Daman site, the estimated C_{HN} value in the first period was lower than that in the other periods. In the first period, the seeded corn was in its early growing stage, and the LAI was low. Additionally, the C_{HN} estimates at the Daman site (a densely vegetated site with large LAI values) are larger than the corresponding estimates at the Huazhaizi site (a sparsely vegetated site with low LAI values). Overall, the results show that the C_{HN} estimates are positively correlated with the vegetation phenology. Although no information on vegetation was used in the WC-VDA scheme, C_{HN} can be well estimated with the sequences of LST observations.

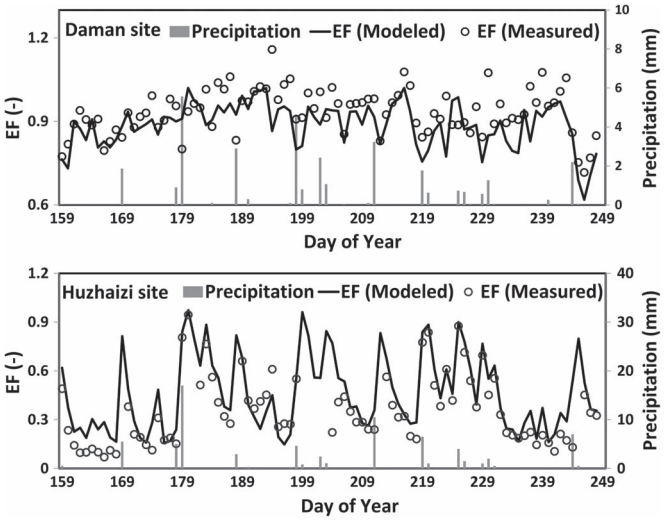

Fig. 1. Evaporative fraction (EF) estimates from the WC-VDA scheme during Julian days 159–248 in the Daman and Huazhaizi sites.

The estimated evaporative fraction (EF) values from the WC-VDA scheme are compared with the EF observations in Fig. 1. The estimated EF values from the model agree well with the observations at the Huazhaizi sites in terms of the magnitude and day-to-day dynamics. The model tends to slightly underestimate EF at the Daman site. When the soil is very wet, the sensible heat flux can become negative. This leads to EF observations larger than unity [see (5)]. However, EF in the WC-VDA scheme is set to be less than 0.97 to prevent numerical instabilities, which causes the EF estimates to be smaller than the observations.

No soil moisture or precipitation data were used in the WC-VDA scheme. However, the estimated EF can capture the wetting and drydown events. For example, at the Huazhaizi site, the estimated EF sharply increases when precipitation occurs (e.g., Julian days 169, 179, 188, 198, 202, 211, 219, 225, 230, and 244). However, after these days, the land surface quickly becomes dry, and the estimated EF decreases accordingly.

Fig. 2 compares the half-hourly turbulent heat flux estimates with the EC measurements at the Daman and Huazhaizi sites. The Daman site is a seeded corn site located in an oasis area with a low sensible heat flux and a high latent heat flux (evapotranspiration and ET), and the Huazhaizi site is a desert site

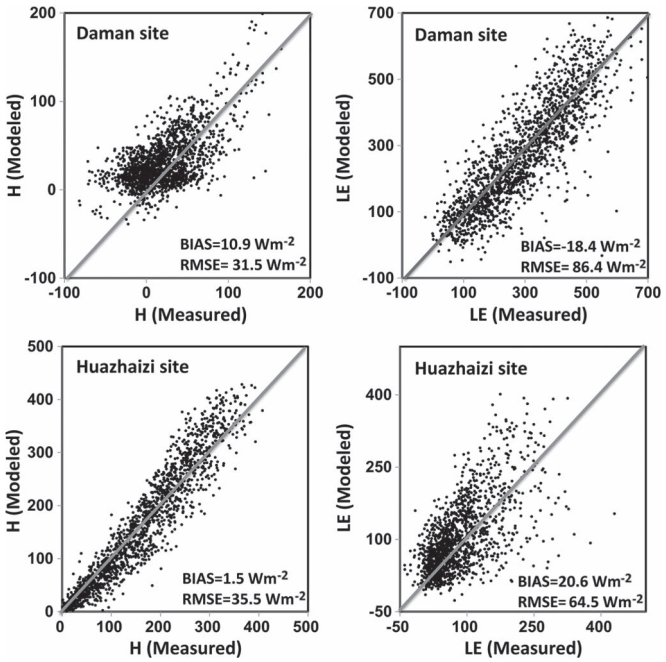

Fig. 2. Comparison between half-hourly modeled and measured sensible and latent heat fluxes in the (top) Daman and (bottom) Huazhaizi sites.

TABLE I
BIAS AND RMSE OF HALF-HOURLY SENSIBLE AND LATENT HEAT FLUX ESTIMATES FROM THE WC-VDA AND SC-VDA SYSTEMS

Site	Approach	H (Wm^{-2})		LE (Wm^{-2})	
		Bias	RMSE	Bias	RMSE
Daman	WC-VDA	10.9	31.5	-18.4	86.4
	SC-VDA	12.5	32.8	-18.6	89.1
Huazhaizi	WC-VDA	1.5	35.5	20.6	64.5
	SC-VDA	3.5	36.1	43.3	80.2

beside the oasis with a high sensible heat flux and a low latent heat flux. Fig. 2 implies that the WC-VDA scheme works well at these two sites with contrasting ecological and hydrological conditions. The estimated sensible and latent heat fluxes (H and LE, respectively) agree well with the EC measurements at both the Daman and Huazhaizi sites, and the scatter plots mainly fall around the 1:1 line. At the Daman site, the bias (RMSE) is 10.9 W $\cdot$ m^{-2} (31.5 W $\cdot$ m^{-2}) for the sensible heat flux and -18.4 W $\cdot$ m^{-2} (86.4 W $\cdot$ m^{-2}) for the latent heat flux. At the Huazhaizi site, the H and LE estimates have a bias of 1.5 W $\cdot$ m^{-2} and a bias of 20.6 W $\cdot$ m^{-2}, respectively. The corresponding RMSEs are 35.5 and 64.5 W $\cdot$ m^{-2}. The statistical metrics indicate that the WC-VDA is a feasible approach for estimating surface heat fluxes.

The performance of the WC-VDA system is compared with that of the SC-VDA approach, and the results are presented in Table I. As shown, the WC-VDA system outperforms the SC-VDA approach and decreases the RMSE of the LE estimates from 89.1 to 86.4 W $\cdot$ m^{-2} at the Daman site and from 80.2 to 64.5 W $\cdot$ m^{-2} at the Huazhaizi site. These results clearly illustrate that incorporating the model error term within the VDA system enables us to account for the structural model errors, the noise in the micrometeorological forcings, and the uncertainties due to the inaccurate specification of input parameters such as soil thermal properties, albedo, etc.

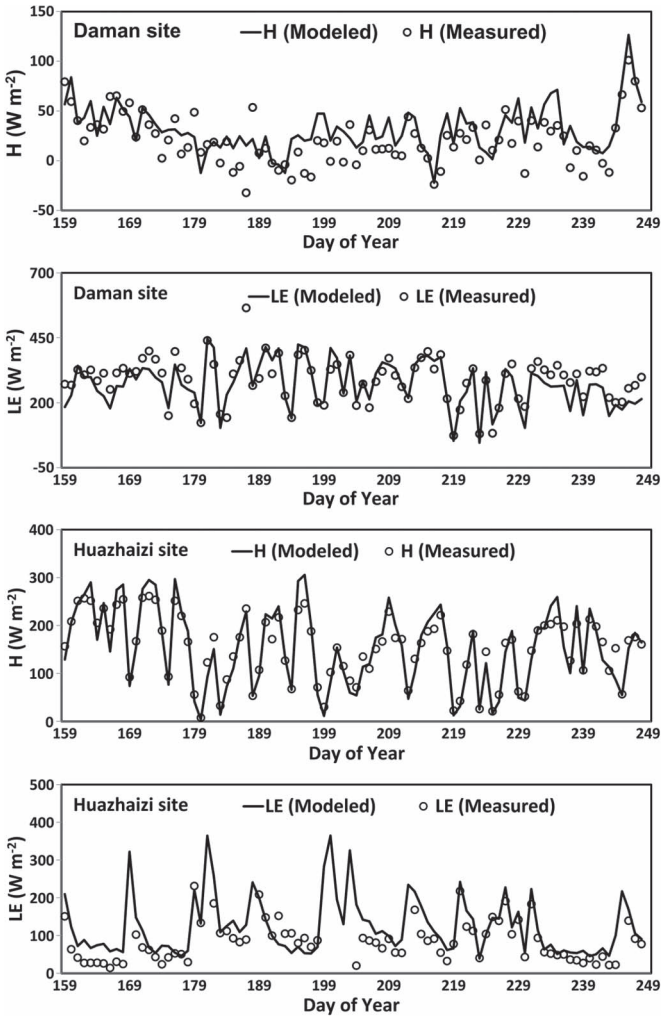

Fig. 3. Daytime-averaged turbulent heat flux estimates from model estimates (the solid line) compared with the ground measurements (the open circles) in the Daman and Huazhaizi sites.

Fig. 3 shows the daytime-averaged (0900–1800) sensible and latent heat flux estimates at the Daman and Huazhaizi sites. The flux observations are also shown in this figure. As illustrated, the estimated turbulent heat fluxes agree with the ground measurements. This figure implies that the WC-VDA scheme can yield reasonable flux estimates with sequences of LST observations. It is worth mentioning that, during Julian days 179–240, the WC-VDA generally overestimates the sensible heat flux at the Daman site.

There are several reasons for the discrepancy between the surface heat flux estimates and the measurements. Soil thermal conductivity (λ) and heat capacity (c) are assumed to be constant during the whole data assimilation period; neutral bulk heat transfer coefficient (C_{HN}) is presumed to be constant every 30 days; and evaporative fraction (EF) is assumed to be constant in each day. In addition, there are uncertainties in the EC-measured sensible and latent heat fluxes. The uncertainties (RMSE) of the EC measurements were accessed during HiWATER-MUSOEXE [3]. The uncertainties (RMSE) of the sensible heat flux are 7.62 W $\cdot$ m^{-2} for the Daman site (No. H5) and 13.4 W $\cdot$ m^{-2} for the Huazhaizi site (No. H14); the corresponding uncertainties (RMSE) in the latent heat

fluxes are 4.36 $\mathrm{W \cdot m^{-2}}$ for the Daman site (No. LE5) and 4.22 $\mathrm{W \cdot m^{-2}}$ for the Huazhaizi site (No. LE14).

V. Conclusion

Turbulent heat fluxes are estimated at the Daman (oasis) and Huazhaizi (desert) sites in the middle reach of the HRB with a WC-VDA scheme. The estimated half-hourly flux estimates agree well with the EC measurements. The bias (RMSE) is 10.9 $\mathrm{W \cdot m^{-2}}$ (31.5 $\mathrm{W \cdot m^{-2}}$) for the sensible heat flux and -18.4 $\mathrm{W \cdot m^{-2}}$ (86.4 $\mathrm{W \cdot m^{-2}}$) for the latent heat flux estimates at the Daman site. At the Huazhaizi site, the biases (RMSEs) of the sensible and latent heat flux estimates are 1.5 $\mathrm{W \cdot m^{-2}}$ (35.5 $\mathrm{W \cdot m^{-2}}$) and 20.6 $\mathrm{W \cdot m^{-2}}$ (64.5 $\mathrm{W \cdot m^{-2}}$), respectively. The changes in the estimated neutral bulk heat transfer coefficients (C_{HN}) for different monthly periods are consistent with variations in vegetation phenology. The evaporative fraction (EF) estimates have day-to-day fluctuations consistent with those of the observations, although no precipitation or soil moisture observations were used in the WC-VDA scheme. One reason for the model estimate errors may be caused by the assumptions of constant soil thermal properties (λ and c) and constant model parameters (C_{HN} and EF) in the WC-VDA scheme. Another reason for the misfit between the model estimates and the observations can be ascribed to measurement errors [3].

Compared with the SC-VDA scheme, an error term that accounts for model errors was added to the VDA scheme. The developed WC-VDA scheme performs well over distinct hydrological and vegetated conditions. Future studies should focus on improving the surface heat flux estimates by assimilating the soil moisture or precipitation data within the WC-VDA scheme.

Acknowledgment

The authors would like to thank all the scientists, engineers, and students who participated in the HiWATER field campaigns. The authors would also like to thank Prof. X. Wen for providing the LAI data used in this letter.

References

[1] S. M. Liu *et al.*, "A comparison of eddy-covariance and large aperture scintillometer measurements with respect to the energy balance closure problem," *Hydrol. Earth. Syst. Sci.*, vol. 15, no. 4, pp. 1291–1306, Apr. 2011.

[2] S. M. Liu, Z. W. Xu, Z. L. Zhu, Z. Z. Jia, and M. J. Zhu, "Measurements of evapotranspiration from eddy-covariance systems and large aperture scintillometers in the Hai River Basin, China," *J. Hydrol.*, vol. 487, pp. 24–38, Apr. 2013.

[3] Z. W. Xu *et al.*, "Intercomparison of surface energy flux measurement systems used during the HiWATER-MUSOEXE," *J. Geophys. Res.*, vol. 118, no. 23, pp. 13140–13157, Dec. 2013.

[4] S. M. Bateni and D. Entekhabi, "Relative efficiency of land surface energy balance components," *Water Resourc. Res.*, vol. 48, no. 4, pp. W04510-1–W04510-8, Apr. 2012.

[5] J. Cheng, "Land surface temperature and thermal infrared emissivity," in *Advanced Remote Sensing: Terrestrial Information Extraction and Applications*, S. Liang, X. Li, and J. Wang, Eds., 1st ed. New York, NY, USA: Academic Press, Apr. 2012, pp. 235–268.

[6] L. Jiang and S. Islam, "Estimation of surface evaporation map over Southern Great Plain using remote sensing data," *Water Resourc. Res.*, vol. 37, no. 2, pp. 329–340, Feb. 2001.

[7] K. Wang, Z. Li, and M. Cribb, "Estimating of evaporative fraction from a combination of day and night land surface temperature and NDVI: A new method to determine the Priestley-Taylor parameter," *Remote Sens. Environ.*, vol. 102, no. 3/4, pp. 293–305, Jun. 2006.

[8] J. M. Norman, W. P. Kustas, and K. Humes, "A two-source approach for estimation of soil and vegetation energy fluxes from observations of directional radiometric surface temperature," *Agr. Forest Meteorol.*, vol. 77, no. 1, pp. 263–293, Apr. 1995.

[9] Z. Su, "The Surface Energy Balance System (SEBS) for estimation of turbulent heat fluxes," *Hydrol. Earth Syst. Sci.*, vol. 6, no. 1, pp. 85–100, 2002.

[10] S. M. Liu, G. Hu, L. Lu, and D. Mao, "Estimation of regional evapotranspiration by TM/ETM+ data over heterogeneous surfaces," *Photogramm. Eng. Remote Sens.*, vol. 73, no. 10, pp. 1169–1178, Oct. 2007.

[11] F. Castelli, D. Entekhabi, and E. Caporali, "Estimation of surface heat transfer and an index of soil moisture using adjoint-state surface energy balance," *Water Resourc. Res.*, vol. 35, no. 10, pp. 3115–3126, Oct. 1999.

[12] G. Boni, D. Entekhabi, and F. Castelli, "Land data assimilation with satellite measurements for the estimation of surface energy balance components and surface control on evaporation," *Water Resourc. Res.*, vol. 37, no. 6, pp. 1713–1722, Jun. 2001.

[13] F. Caparrini, F. Castelli, and D. Entekhabi, "Mapping of land atmosphere heat fluxes and surface parameters with remote sensing data," *Boundary Layer Meteorol.*, vol. 107, no. 3, pp. 605–633, Jun. 2003.

[14] F. Caparrini, F. Castelli, and D. Entekhabi, "Estimation of surface turbulent fluxes through assimilation of radiometric surface temperature sequences," *J. Hydrometeorol.*, vol. 5, no. 1, pp. 145–159, Feb. 2004.

[15] W. T. Crow and W. P. Kustas, "Utility of assimilating surface radiometric temperature observations for evaporative fraction and heat transfer coefficient retrieval," *Boundary-Layer Meteorol.*, vol. 115, no. 1, pp. 105–130, Apr. 2005.

[16] J. Qin, S. Liang, R. Liu, H. Zhang, and B. Hu, "A weak-constraint based data assimilation scheme for estimating surface turbulent fluxes," *IEEE Geosci. Remote Sens. Lett.*, vol. 4, no. 4, pp. 649–653, Oct. 2007.

[17] F. Sini, G. Boni, F. Caparrini, and D. Entekhabi, "Estimation of large-scale evaporation fields based on assimilation of remotely sensed land temperature," *Water Resourc. Res.*, vol. 44, no. 6, pp. W06410-1–W06410-15, Jun. 2008.

[18] S. M. Bateni, D. Entekhabi, and D. S. Jeng, "Variational assimilation of land surface temperature and the estimation of surface energy balance components," *J. Hydrol.*, vol. 481, pp. 143–156, Feb. 2013.

[19] S. M. Bateni and S. Liang, "Estimating surface energy fluxes using a dual-source data assimilation approach adjoined to the heat diffusion equation," *J. Geophys. Res.*, vol. 117, no. D17, pp. D17118-1–D17118-13, Sep. 2012.

[20] S. M. Bateni, D. Entekhabi, and F. Castelli, "Mapping evaporation and estimation of surface control of evaporation using remotely sensed land surface temperature from a constellation of satellites," *Water Resourc. Res.*, vol. 49, no. 2, pp. 950–968, Feb. 2013.

[21] T. R. Xu, S. Liang, and S. M. Liu, "Estimating turbulent fluxes through assimilation of geostationary operational environmental satellites data using ensemble Kalman filter," *J. Geophys. Res.*, vol. 116, no. D9, pp. D09109-1–D09109-16, May 2011.

[22] T. R. Xu, S. M. Liu, S. Liang, and J. Qin, "Improving predictions of water and heat fluxes by assimilating MODIS land surface temperature products into the common land model," *J. Hydrometeorol.*, vol. 12, no. 2, pp. 227–244, Apr. 2011.

[23] Z. Hu and S. Islam, "Prediction of ground temperature and soil moisture content by the force-restore method," *Water Resourc. Res.*, vol. 31, no. 10, pp. 2531–2539, Oct. 1995.

[24] P. Gentine, D. Entekhabi, and A. Chehbouni, "Analysis of evaporative fraction diurnal behavior," *Agr. Forest Meteorol.*, vol. 143, no. 1/2, pp. 13–29, Mar. 2007.

[25] S. Margulis and D. Entekhabi, "Variational assimilation of surface temperature and micrometeorology into a model of the atmospheric boundary layer and land surface," *Mon. Weather Rev.*, vol. 131, no. 7, pp. 1272–1288, Jul. 2003.

[26] R. H. Reichle, "Data assimilation methods in the earth sciences," *Adv. Water. Resourc.*, vol. 31, no. 11, pp. 1411–1418, Nov. 2008.

[27] X. Li *et al.*, "Heihe Watershed Allied Telemetry Experimental Research (HiWATER): Scientific objectives and experimental design," *Bull. Amer. Meteorol. Soc.*, vol. 94, no. 8, pp. 1145–1160, Aug. 2013.

[28] M. G. Ma *et al.*, "HiWATER: Dataset of soil parameters in the middle reaches of the Heihe River Basin," Heihe Plan Science Data Center, 2013.

[29] D. A. de Vries, "Thermal properties of soils," in *Physics of Plant Environment*, W. R. van Wijk, Ed. Amsterdam, The Netherlands: North Holland, 1963, pp. 210–235.

[30] O. T. Farouki, "The thermal properties of soils in cold regions," *Cold Regions Sci. Technol.*, vol. 5, no. 1, pp. 67–75, Sep. 1981.